targets

MDPI

Article

Pharmacological Profiling of Cannabinoid CB_2 Receptor Ligands in Non-Stimulated BV-2 Microglia Cells

Pietro Marini [1,*], Guy S. Bewick [2], Maria Grazia Morgese [3], Stefania Schiavone [3] and Paolo Tucci [3]

[1] Institute of Education in Healthcare and Medical Sciences, Foresterhill Campus, University of Aberdeen, Aberdeen AB25 2ZD, UK
[2] Institute of Medical Sciences, Foresterhill Campus, University of Aberdeen, Aberdeen AB25 2ZD, UK; g.s.bewick@abdn.ac.uk
[3] Department of Clinical and Experimental Medicine, University of Foggia, 71122 Foggia, Italy; mariagrazia.morgese@unifg.it (M.G.M.); stefania.schiavone@unifg.it (S.S.); paolo.tucci@unifg.it (P.T.)
* Correspondence: p.marini@abdn.ac.uk

Abstract

Microglia are key regulators of central nervous system homeostasis and neuroinflammation, and cannabinoid type 2 receptors (CB_2Rs) have emerged as important modulators of microglial function. Although the pharmacology of CB_2Rs has been extensively characterised in heterologous expression systems and activated microglia, comparatively little is known about the behaviour of CB_2R ligands in non-stimulated microglia. The present study therefore aimed to characterise the pharmacological properties of a panel of CB_2R ligands in non-stimulated BV-2 microglial cells and to determine whether constitutive receptor activity and ligand-dependent signalling bias could be detected under basal conditions. Classical CB_2R agonists (CP 55,940, WIN 55,212-2, JWH 133 and JWH 015), putative protean agonists ((R)-AM 1241 and GW 405833), and inverse agonists (SR 144528, AM 630 and JTE 907) were evaluated using [^{35}S]GTPγS binding and forskolin-stimulated cAMP assays. In the [^{35}S]GTPγS assay, WIN 55,212-2 displayed the highest intrinsic activity, whereas (R)-AM 1241 and GW 405833 behaved as partial agonists. Inverse agonists reduced basal signalling, indicating constitutive CB_2R activity in resting BV-2 cells. In contrast, cAMP measurements revealed greater signal amplification, with (R)-AM 1241 and GW 405833 exhibiting full agonist behaviour and SR 144528 producing pronounced inverse agonism. Marked differences in ligand efficacy and rank order between assays highlighted the influence of downstream signalling mechanisms and ligand-dependent signalling bias. Notably, GW 405833 displayed a strongly biased signalling profile, whereas SR 144528 consistently exhibited the greatest inverse agonist activity. These findings demonstrate that CB_2Rs are functionally active in non-stimulated microglia and that constitutive receptor activity and signalling bias contribute significantly to their pharmacological profile under basal conditions. By focusing on non-stimulated microglia, this study provides new insights into CB_2R signalling in a homeostatic cellular environment and establishes a framework for understanding how CB_2R pharmacology may be altered during neuroinflammatory and neurodegenerative disease states.

Keywords: BV2 cells; microglia; CB_2 receptors; cAMP; [^{35}S]GTPγS

Academic Editor: Huangxian Ju

Received: 20 July 2026
Revised: 18 August 2026
Accepted: 31 August 2026
Published: 2 September 2026

1. Introduction

Microglia are specialized resident immune cells of the central nervous system (CNS) that continuously surveil the neural environment, protect against infectious agents, con-

tribute to tissue repair, and participate in synaptic pruning during brain development. In addition to their protective functions, which involve the release of reactive oxygen and nitrogen species and a variety of inflammatory mediators, microglia can also exert detrimental effects on neuronal cells under pathological conditions [1]. Thus, microglia perform numerous important functions that may be targeted therapeutically, including inflammatory signalling, phagocytosis, synaptic pruning, triggering receptor expressed on myeloid cells 2 (TREM2)-mediated disease responses, purinergic signalling and surveillance, as well as microglial proliferation and survival [2].

Homeostatic microglia are generally considered to exhibit an M0 phenotype [3]. Microglial activation is commonly classified into two additional functional states: the classical pro-inflammatory activation state (M1 phenotype), which exerts both protective and potentially neurotoxic effects, and the alternative anti-inflammatory activation state (M2 phenotype), which promotes tissue repair, neuronal recovery, and the resolution of inflammation [2]. The transition from the M1 to the M2 phenotype is influenced by microenvironmental factors associated with different central nervous system (CNS) pathologies and stages of disease progression. Consequently, considerable research efforts have focused on identifying the cellular mechanisms that regulate this phenotypic switch. Among the pathways implicated in this process, the cannabinoid type 2 receptor (CB_2R), which is highly expressed in activated microglia, has been proposed as a key regulator of microglial phenotype switching [4–6].

Similar to peripheral immune cells, homeostatic microglia (M0 phenotype) express very low levels of CB_2R mRNA [7]. Upon microglial activation, CB_2R expression is markedly modulated in a stimulus-dependent manner and is generally upregulated under reactive and neuroinflammatory conditions [8]. This increase has been proposed as a potential biomarker of neuroinflammation associated with several CNS disorders [2,9–11]. Notably, CB_2R upregulation is not restricted to the pro-inflammatory (M1) phenotype. Activation of CB_2R also promotes and accompanies anti-inflammatory (M2) polarisation, and the direction of its regulation depends on the specific inflammatory stimulus [8].

Despite the relatively low basal expression of CB_2R in non-stimulated microglia, several studies have demonstrated the presence of functional CB_2 receptors in BV-2 cells and other microglial preparations [12,13]. Furthermore, evaluating CB_2R pharmacology in non-stimulated microglia is essential for establishing the receptor's baseline signalling properties in a native, non-stimulated cellular environment, in which changes in CB_2R expression and/or function have not yet been induced. Such information is particularly relevant for compounds displaying context-dependent efficacy, including ligands that exhibit protean agonism or inverse agonism. Depending on CB_2R density and/or constitutive activity, protean ligands may induce different receptor responses. Characterisation of CB_2R ligands in non-stimulated BV-2 cells would provide an important reference framework for understanding how activation-dependent alterations or changes in the cellular environment may influence CB_2R signalling.

In addition to expressing cannabinoid receptors, microglia are capable of synthesizing and degrading endocannabinoids (eCBs), thereby contributing to the regulation of the endocannabinoid system within the CNS [6]. Over the last decade, numerous in vitro studies have demonstrated an important role for the endocannabinoid system in modulating microglial polarization and regulating neuroinflammatory processes, with CB_2R activation being a major contributor to centrally mediated anti-inflammatory responses and as regulator of microglial phenotype [14–17]. By contrast, its role in animal models remains not fully understood due to the complexity of the numerous regulatory mechanisms operating within the CNS [5].

These findings suggest that CB_2R may represent a promising pharmacological target for the treatment of CNS disorders in which microglial dysfunction contributes to disease pathogenesis [18]. Following the cloning and characterization of the CB_2R [19], numerous receptor ligands have been identified. Similar to other G protein-coupled receptors (GPCRs), CB_2R exhibits variable constitutive activity when expressed in vitro and/or in vivo [20]. This characteristic is known to influence the pharmacological properties of CB_2R ligands; therefore, a model-specific approach is required for their characterisation [21]. When evaluated in recombinant systems, which typically exhibit high CB_2R density and constitutive activity, and in naturally expressing systems, which generally display lower receptor density and constitutive activity, some compounds have shown so-called functional activity, behaving as agonists, inverse agonists, or antagonists while binding to CB_2R [18]. Ligands displaying these atypical pharmacological behaviours are currently classified as protean agonists. Briefly, a protean agonist is characterized by its ability to produce agonist effects in systems with low constitutive receptor activity while exhibiting inverse agonist effects in systems with high constitutive receptor activity [22]. It has been proposed that protean agonists can stabilize receptors in distinct conformational states, promoting a shift between active and inactive receptor conformations depending on the experimental conditions employed [23]. Evidence supporting this concept has been reported for the CB_2 receptor ligand AM 630, which behaves as a protean ligand at the human CB_2 receptor [23,24]. An example of this phenomenon is also provided by the selective CB_2R ligands (R)-AM 1241 and GW 405833 (also known as L-768,242). In recombinant systems, both compounds have been reported to behave as inverse agonists, whereas in naturally expressing systems, (R)-AM 1241 behaved as a full agonist and GW 405833 as a partial agonist [21,25,26]. Investigations conducted in naturally expressing systems, including mouse, rat, and human spleen membranes, have also demonstrated functional activity for the CB_2R agonists JWH 015 and JWH 133, as well as for the CB_2R inverse agonists SR 144528, AM 630, and JTE 907 [21]. To further characterise the pharmacology of CB_2R ligands in naturally expressing models, the murine BV-2 microglial cell line represents a useful experimental system. This cellular model is widely employed for in vitro studies of microglial function in the CNS and is also commonly used to investigate the endocannabinoid system, as its components are expressed in both BV-2 cells [3,27] as well as in primary glial cells [28,29].

In the present study, we characterised the pharmacological properties of a series of well-established CB_2R ligands in BV-2 cells using cyclic AMP accumulation and [^{35}S]GTPγS binding assay [30].

Whereas the [^{35}S]GTPγS binding assay measures receptor-induced G-protein activation directly, the cAMP assay evaluates a downstream functional response. It is therefore particularly useful for assessing the ability of CB_2R ligands to modulate adenylyl cyclase activity and for detecting differences in ligand efficacy that may not be evident at the level of G-protein activation [31]. As reference compounds, we examined the effects of CP 55,940, a highly potent cannabinoid ligand with high affinity for both CB_1R and CB_2R [32], and WIN 55,212-2, a potent cannabinoid receptor agonist active at both receptor subtypes, with a modest preference for CB_2R [21,33]. Through these studies, we aimed to better define the pharmacological profile of CB_2R ligands in non-stimulated microglial cells.

2. Materials and Methods

2.1. Culturing and Treatment of Cells

The murine microglial cell line BV-2 (Cambridge Bioscience, Cambridge, Cambridgeshire, UK) was cultured in DMEM supplemented with 3% foetal bovine serum (FBS), 10 mM HEPES, 5 mM $NaHCO_3$, penicillin (100 U/mL), and streptomycin (100 µg/mL) (Sigma-Aldrich, Poole, Dorset, UK). Cells were maintained at 37 °C in a humidified at-

mosphere containing 5% CO_2 and passaged every 3 to 4 days for up to 12 passages. Approximately 24 h before the experiments, BV-2 cells were harvested for the cAMP assay and seeded into 96-well plates at a volume of 100 µL per well. Membranes for the [^{35}S]GTPγS binding assay were prepared from the same batch of cells. All experiments were performed using independent preparations generated from separate BV-2 cell cultures maintained under identical conditions, within the permitted passage range and at the same passage number (passages 7–8). The minimum of three independent replicates reported throughout the study therefore represents biological replicates derived from independent membrane preparations, rather than technical replicates obtained from a single preparation. Cannabinoid compounds were dissolved in DMSO as 1000× stock solutions using siliconized glass vials and siliconized pipette tips (Sigma-Aldrich, Poole, Dorset, UK).

2.2. Membrane Preparation for [^{35}S]GTPγS Binding Assays

BV-2 cells were detached from culture flasks by scraping, collected by centrifugation, and stored as cell pellets at −20 °C until use. Prior to the [^{35}S]GTPγS binding assay, cell pellets were thawed in 50 mM Tris buffer (pH 7.4) and homogenized using a handheld homogenizer fitted with a 1 mL probe. Protein concentrations were determined using the Bio-Rad DC Protein Assay Kit (Bio-Rad Laboratories Ltd., Hemel Hempstead, Hertfordshire, UK).

2.3. [^{35}S]GTPγS-Binding Assays

Measurement of ligand-stimulated [^{35}S]GTPγS binding to cannabinoid CB_2 receptors was adapted from previously described methods [34,35]. Assays were performed in GTPγS binding buffer containing 50 mM Tris-HCl, 50 mM Tris-base, 5 mM $MgCl_2$, 1 mM ethylenediaminetetraacetic acid (EDTA), 100 mM NaCl, 1 mM dithiothreitol (DTT), and 0.1% bovine serum albumin (BSA) (Sigma-Aldrich, Poole, Dorset, UK), in the presence of [^{35}S]GTPγS (Revvity, Waterbeach, Cambridge, UK) and GDP (Sigma-Aldrich, Poole, Dorset, UK), in a final volume of 500 µL. Binding reactions were initiated by the addition of [^{35}S]GTPγS. Non-specific binding was determined in the presence of 30 µM unlabelled GTPγS (Sigma-Aldrich, Poole, Dorset, UK). Test compounds were incubated for 60 min at 30 °C. Reactions were terminated by rapid vacuum filtration using Tris binding buffer, as previously described [21], and retained radioactivity was quantified by liquid scintillation spectrometry. Unless otherwise stated, all [^{35}S]GTPγS binding assays were performed using 0.1 nM [^{35}S]GTPγS, 30 µM GDP, and 40 µg of BV-2 membrane protein per well. All compounds were dissolved in DMSO and stored at −20 °C until use.

2.4. Cyclic AMP (cAMP) Assay

Intracellular cAMP levels were measured using the HitHunter® cAMP assay kit (Eurofins DiscoverX Products, Celle-L'Évescault, France) according to the manufacturer's instructions and as previously described [21,36]. Briefly, BV-2 cells were detached using a cell dissociation buffer, counted, and seeded at a density of 2×10^4 cells per well in 100 µL of complete culture medium in white 96-well plates. Cells were then incubated at 37 °C in a humidified atmosphere containing 5% CO_2 for approximately 24 h before the assay.

Assay and drug dilutions were prepared in a 1:1 mixture of DMEM and Ham's F-12 medium without phenol red, supplemented with 10 µM rolipram and forskolin (FSK) (Sigma-Aldrich, Poole, Dorset, UK).

Forskolin (10 µM) was used to stimulate adenylyl cyclase and generate a robust increase in intracellular cAMP levels, thereby providing a suitable dynamic range for detecting CB_2R-mediated inhibition of cAMP accumulation. Rolipram (10 µM) was included to inhibit phosphodiesterase-4 activity and prevent cAMP degradation, thereby increasing assay sensitivity and reproducibility. These concentrations are commonly employed

in studies investigating signalling through $G_{i/o}$-coupled receptors and were selected to provide a stable and quantifiable cAMP response against which the effects of CB_2R ligands could be assessed [21,36,37].

Prior to treatment, the culture medium was removed, and cells were washed with DMEM/F-12 medium (Sigma-Aldrich, Poole, Dorset, UK). Cells were then exposed to the test compounds (30 µL per well) and incubated for 30 min at 37 °C in a humidified atmosphere containing 5% CO_2.

Subsequently, cAMP standards and the appropriate detection reagents were added according to the manufacturer's instructions (Eurofins DiscoverX Products, Celle-L'Évescault, France). Plates were incubated overnight at room temperature in the dark. Chemiluminescent signals were measured using a Synergy HT Multi-Mode Microplate Reader (BioTek Instruments, Winooski, VT, USA).

2.5. Cannabinoid Compounds

WIN 55,212-2, CP 55,940, JWH 133, JWH 015, (R)-AM 1241, AM 630, SR 144528, GW 405833, JTE 907, were obtained from Cayman Chemical (Ann Arbor, MI, USA).

2.6. Statistical Analysis

Concentration-response curves for the [^{35}S]GTPγS binding and cAMP assays were analysed using GraphPad Prism 5.04 (GraphPad Software, San Diego, CA, USA). Data were analysed directly from the experimental measurements and were not normalised prior to curve fitting. Agonist and inverse agonist responses (EC_{50} values and maximal [^{35}S]GTPγS binding or FSK-induced cAMP production) were fitted using a four-parameter logistic equation and analysed by nonlinear regression. Basal [^{35}S]GTPγS binding was determined in the absence of ligand and served as the reference level for calculating ligand-induced changes in binding. Consequently, compounds that produced responses below basal binding exhibited negative efficacy values, consistent with inverse agonist activity and a reduction in constitutive receptor signalling. Data are expressed as means, and variability is reported as either the standard error of the mean (S.E.M.) or 95% confidence intervals (CIs), as indicated in the text.

3. Results

3.1. Efficacies and Potencies of Putative CB_2 Receptor Agonists: CP 55,940, WIN 55,212-2, JWH 133, JWH 015 in the [^{35}S]GTPγS Assay

In the [^{35}S]GTPγS binding assay among the compounds tested, WIN 55,212-2 behaved as a full agonist in BV-2 cell membranes, exhibiting the highest efficacy (E_{max} = 34.17 ± 1.48%) and potency (EC_{50} = 4.30 nM). CP 55,940 and JWH 133 displayed similar potencies, with EC_{50} values of 13.66 nM and 16.68 nM, respectively. CP 55,940 showed similar efficacy to WIN 55,212-2 (E_{max} = 30.10 ± 2.16) whereas JWH 133 exhibited significantly lower efficacy (E_{max} = 14.56 ± 1.87%). Finally, JWH 015 was the less potent agonist with an EC_{50} value of 33.00 nM, and an intermediate efficacy (E_{max} = 20.70 ± 3.41%) between CP 55,940 and JWH 133 (Table 1; Figure 1).

3.1.1. Efficacies and Potencies CB_2 Receptor 'Protean' Agonists (R)-AM 1241 and GW 405833 in the [^{35}S]GTPγS Assay

Both CB_2 receptor 'protean agonists', (R)-AM 1241 and GW 405833, acted as agonists in BV-2 cells, displaying EC_{50} values of 52.24 nM and 128.50 nM, respectively. Nevertheless, both compounds produced significantly lower E_{max} values than the reference agonists CP 55,940 and WIN 55,212-2 (Table 1; Figure 1).

Table 1. Effect of CB_2 receptor agonists and protean agonists in the [^{35}S]GTPγS binding assay using BV-2 cells. pEC_{50} and E_{max} (maximum response, %) with S.E.M. and EC_{50}, pEC_{50} and E_{max} values with 95% C.I. were determined from GraphPad Prism.

Compound	EC_{50} (nM)	EC_{50} 95% C.I.	$pEC_{50} \pm$ S.E.M.	pEC_{50} 95% C.I.	$E_{max} \pm$ S.E.M.	E_{max} 95% C.I.
WIN 55,212-2	4.30	2.57–16.0	8.37 ± 0.11	8.60–8.14	34.17 ± 1.48	31.21–37.12
CP 55,940	13.66	6.61–28.25	7.86 ± 0.28	8.18–7.55	30.10 ± 2.16	25.79–34.41
JWH 133	16.68	4.58–60.69	7.79 ± 0.28	8.34–7.22	14.56 ± 1.87	10.82–18.30
JWH 015	33.00	6.58–158.80	7.48 ± 0.34	8.16–6.80	20.70 ± 3.41	13.88–27.52
(R)-AM 1241	52.24	13.05–209.10	7.28 ± 0.30	7.88–6.68	23.73 ± 3.78	16.18–31.28
GW 405833	128.50	20.15–819.80	6.89 ± 0.40	7.67–6.08	12.90 ± 3.32	6.28–19.51

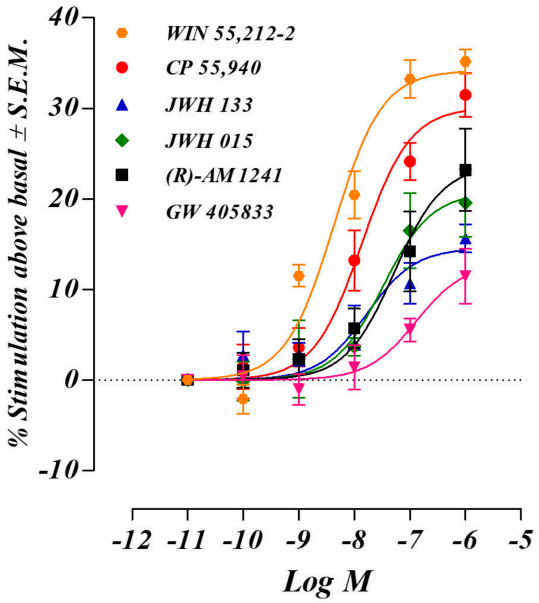

Figure 1. Concentration–response curves of CB_2 receptor ligands WIN 55,212-2, CP 55,940, JWH 133 and JWH 015, (R)-AM 1241 and GW 405833, on [^{35}S]GTPγS binding. Data are expressed as the percentage stimulation of specific [^{35}S]GTPγS binding above the unstimulated basal level. Each point represents the mean ± S.E.M. of independent experiments performed in duplicate (n = 3).

3.1.2. Efficacies and Potencies of CB_2 Receptor Inverse Agonists: SR 144528, AM 630 and JTE 907 in [^{35}S]GTPγS Assay

All these compounds displayed negative E_{max} values, with no significant differences observed among them. These negative efficacy values obtained in the [^{35}S]GTPγS binding assay represent a reduction in basal G-protein activity below the unstimulated level and are therefore indicative of inverse agonist activity. SR 144528 was the most potent compound (EC_{50} = 1.06 nM,), followed by JTE 907 (EC_{50} = 1.81 nM) and AM 630 (EC_{50} = 15.58 nM) (Table 2; Figure 2).

Table 2. Effect of CB_2 receptor inverse agonists in the [^{35}S]GTPγS binding assay using BV-2 cells. pEC_{50} and E_{max} (maximum response, %) with S.E.M. and EC_{50}, pEC_{50} and E_{max} values with 95% C.I. were determined from GraphPad Prism.

Compound	EC_{50} (nM)	EC_{50} 95% C.I.	$pEC_{50} \pm$ S.E.M.	pEC_{50} 95% C.I.	$E_{max} \pm$ S.E.M.	E_{max} 95% C.I.
SR 144528	1.06	0.41–2.72	8.97 ± 0.20	9.38–8.56	−13.38 ± 1.00	−15.38–−11.38
JTE 907	1.81	0.71–4.58	8.74 ± 0.20	9.14–8.34	−12.69 ± 0.94	−14.57–−10.80
AM 630	15.58	6.78–35.82	7.81 ± 0.18	8.17–7.45	−15.02 ± 1.24	−17.50–−12.54

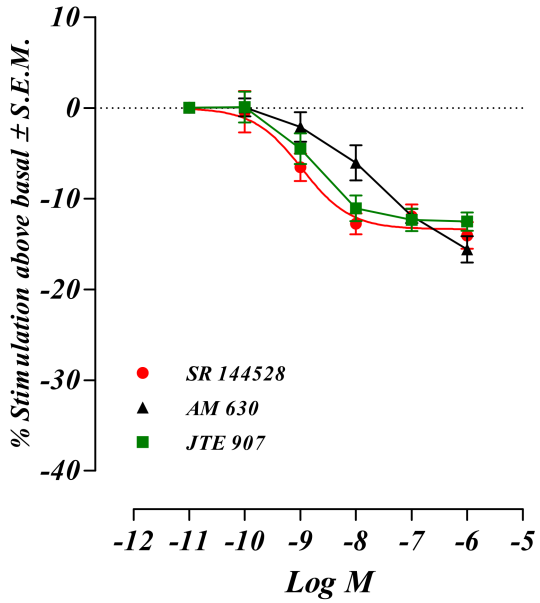

Figure 2. Concentration–response curves of CB_2 receptor ligands SR 144528, AM 630 and JTE 907 on [^{35}S]GTPγS binding. Data are expressed as the percentage stimulation of specific [^{35}S]GTPγS binding below the unstimulated basal level. Each point represents the mean ± S.E.M. of independent experiments performed in duplicate (n = 3).

3.2. Efficacies and Potencies of CB_2 Receptor Agonists: CP 55,940, WIN 55,212-2, JWH 133, JWH 015 in cAMP Assay

The efficacy (E_{max}) of WIN 55,212-2, CP 55,940, JWH 133, and JWH 015 was higher than that measured in the [^{35}S]GTPγS binding assay (68.22 ± 1.74%, 60.03 ± 3.41%, 47.94 ± 2.91%, and 39.68 ± 2.91%, respectively). Although the rank order of efficacy was maintained across assays, the greater maximal responses observed here suggest that receptor activation was translated into a more pronounced downstream functional effect than that detected at the level of G-protein coupling. This observation may be indicative of signal amplification mechanisms operating downstream of CB_2 receptor activation (Table 3; Figure 3).

3.2.1. Effects of CB_2 Receptor 'Protean' Agonists (R)-AM 1241 and GW 405833 in cAMP Assay

In contrast to the [^{35}S]GTPγS binding assay, the 'protean ligands' behaved as full agonists in the cAMP assay, displaying potencies and efficacies comparable to those of the classical ligands described above. Specifically, (R)-AM 1241 exhibited an EC_{50} value of 7.57 nM and an E_{max} value of 52.37 ± 2.40, while GW 405833 displayed an EC_{50} value of 5.04 nM and an E_{max} value of 61.93 ± 3.27. (Table 3; Figure 3).

Table 3. Effect of CB_2 receptor agonists and protean agonists in the cAMP assay using BV-2 cells. pEC_{50} and E_{max} (maximum response, %) with S.E.M. and EC_{50}, pEC_{50} and E_{max} values with 95% C.I. were determined from GraphPad Prism.

Compound	EC_{50} (nM)	EC_{50} 95% C.I.	pEC_{50} ± S.E.M.	pEC_{50} 95% C.I.	E_{max} ± S.E.M.	E_{max} 95% C.I.
WIN 55,212-2	16.29	11.87–23.35	7.79 ± 0.07	7.92–7.65	68.22 ± 1.74	64.76–71.67
CP 55,940	145.90	82.53–257.80	6.84 ± 0.12	7.08–6.59	60.03 ± 3.41	53.27–66.79
JWH 133	8.99	4.27–18.94	8.05 ± 0.16	8.37–7.72	47.94 ± 2.91	42.35–53.53
JWH 015	13.19	5.30–32.99	7.88 ± 0.20	8.27–7.48	39.68 ± 2.91	33.90–45.47
(R)-AM 1241	7.57	4.18–13.70	8.12 ± 0.13	8.38–7.86	52.37 ± 2.40	47.59–57.14
GW 405833	5.04	2.47–10.36	8.30 ± 0.16	8.61–7.98	61.93 ± 3.27	55.45–68.48

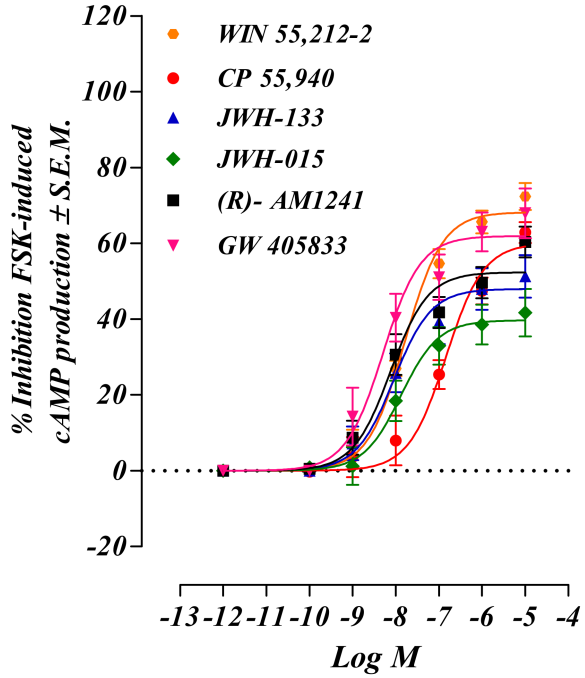

Figure 3. Effects of CB_2 receptor ligands on forskolin-stimulated cAMP production in BV-2 cells. Concentration–response curves for WIN 55,212-2, CP 55,940, JWH 133, JWH 015, (R)-AM 1241 and GW 405833 are shown as percentage inhibition of forskolin (FSK)-induced cAMP accumulation. The concentration of FSK used in these experiments was 10 μM. Each point represents the mean ± S.E.M. of independent experiments performed in duplicate (n = 3).

3.2.2. Effects of CB_2 Receptor Inverse Agonists SR 144528, AM 630 and JTE 907 in cAMP Assay

When tested in the cAMP assay, all compounds induced pronounced negative E_{max} values, indicative of robust inverse agonist activity. However, notable differences were observed in their potency and maximal inverse responses. JTE 907 was the most potent inverse agonist (EC_{50} = 1.10 nM) and displayed an intermediate inverse efficacy (E_{max} = −42.62 ± 2.31%). In contrast, AM 630 exhibited intermediate potency (EC_{50} = 7.35 nM) but the lowest inverse efficacy (E_{max} = −27.41 ± 2.51%). Interestingly, SR 144528 displayed the lowest potency (EC_{50} = 141.80 nM) yet produced the greatest inverse efficacy (E_{max} = −77.90 ± 5.60%) (Table 4; Figure 4). These findings suggest that potency and inverse efficacy were not directly correlated in this assay, as ligands producing the largest maximal responses were not necessarily the most potent. This divergence may reflect differences in the ability of individual compounds to stabilize inactive receptor conformations and suppress constitutive CB_2 receptor signalling.

Table 4. Effect of CB_2 receptor antagonists/inverse agonists in the cAMP assay in BV-2 cells. pEC_{50} and E_{max} (maximum response, %) with S.E.M. and EC_{50}, pEC_{50} and E_{max} values with 95% C.I. were determined from GraphPad Prism.

Compound	EC_{50} (nM)	EC_{50} 95% C.I.	pEC_{50} ± S.E.M.	pEC_{50} 95% C.I.	E_{max} ± S.E.M.	E_{max} 95% C.I.
SR 144528	141.80	69.45–289.50	6.85 ± 0.16	7.16–6.54	−77.90 ± 5.60	−88.88–−66.92
JTE 907	1.10	0.51–2.36	8.96 ± 0.17	9.26–8.62	−42.62 ± 2.31	−47.16–−38.09
AM 630	7.35	2.27–23.73	8.13 ± 0.26	8.64–7.62	−27.41 ± 2.51	−32.33–−22.49

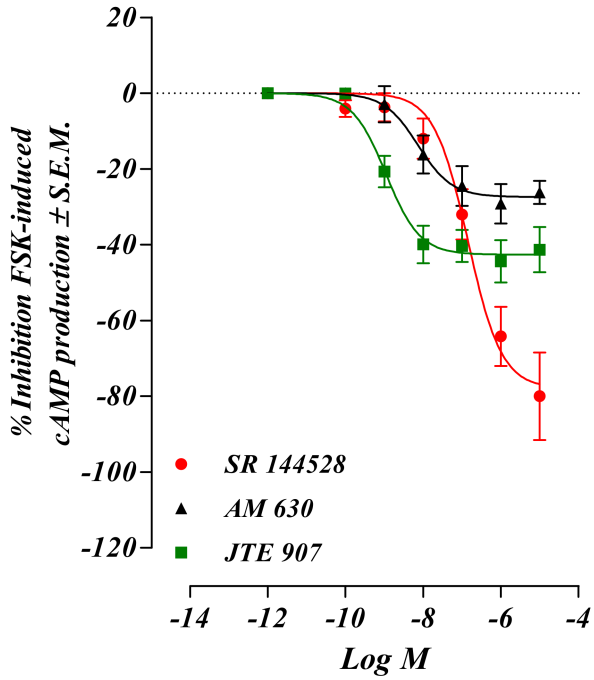

Figure 4. Effects of CB_2 receptor ligands on FSK-stimulated cAMP production in BV-2 cells. Concentration–response curves for SR 144528, AM 630 and JTE 907 are shown as percentage inhibition of FSK-induced cAMP accumulation. The concentration of forskolin used in these experiments was 10 μM. Each point represents the mean ± S.E.M. of independent experiments performed in duplicate (n = 3).

4. Discussion

At G protein-coupled receptors (GPCRs), including the CB_2 receptor studied here, EC_{50} values from the [^{35}S]GTPγS binding assay reflect both ligand potency and efficacy. This assay enables determination of classical pharmacological parameters, including potency, efficacy, and antagonist affinity, without the confounding influence of downstream signal amplification or regulatory mechanisms [38]. Comparison with forskolin (FSK)-stimulated cAMP measurements therefore provides insight into the contribution of downstream signalling to functional responses. Consistent with this, CP 55,940, WIN 55,212-2, JWH 133, and JWH 015 produced greater maximal responses (E_{max}) in the cAMP assay than in the [^{35}S]GTPγS assay.

This pattern agrees with findings in recombinant Chinese hamster ovary (CHO) cells [39]. However, CP 55,940 showed markedly lower potency in the cAMP assay in BV-2 microglial cells than in recombinant CHO systems, suggesting that its pharmacological profile is influenced by cellular context [39]. A possible contributor to this atypical profile is the reported activity of CP 55,940 at GPR55 receptors, which are also expressed in BV-2 cells [40].

Although GPR55-mediated interference in the [^{35}S]GTPγS binding assay is likely to be minimal, given that GPR55 predominantly couples to $G_{12/13}$ proteins while this assay primarily detects $G_{i/o}$ activation [40], cAMP measurements are more vulnerable to downstream signalling crosstalk and receptor-dependent regulatory influences [41]. Therefore, the reduced potency of CP 55,940 in the cAMP assay may reflect the contribution of GPR55 signalling and/or other microglia-specific modulatory pathways that are not evident in assays that directly assess G-protein activation. Collectively, these findings suggest that receptor interactions and downstream signalling networks may significantly influence cannabinoid ligand activity in microglia, potentially contributing to the assay-dependent differences observed for CP 55,940.

Downstream signal amplification appeared particularly relevant for (R)-AM 1241 and GW 405833. Both compounds behaved as partial agonists in the [^{35}S]GTPγS assay but produced full agonist responses in the cAMP assay, supporting their classification as protean agonists in BV-2 microglial cells.

Although the E_{max}/EC_{50} ratio is an imperfect measure of intrinsic efficacy, since it is influenced by both efficacy and affinity, it nevertheless provides a useful parameter for comparing relative ligand activity across different assay platforms [42,43].

Analysis of intrinsic relative activity (see Supplementary Materials) revealed marked assay-dependent changes in ligand rank order. WIN 55,212-2 showed the highest activity in the [^{35}S]GTPγS assay (E_{max}/EC_{50} = 8.01) but ranked fourth in the cAMP assay (E_{max}/EC_{50} = 4.21). CP 55,940 showed the lowest activity in the cAMP assay (E_{max}/EC_{50} = 0.42), mainly due to an approximately ten-fold increase in EC_{50}, suggesting reduced coupling efficiency between receptor activation and inhibition of cAMP accumulation. Similar discrepancies have not been reported in recombinant systems expressing murine or human CB_2 receptors, supporting the presence of microglia-specific regulatory mechanisms and highlighting the importance of studying CB_2R pharmacology in physiologically relevant models.

In contrast to CP 55,940, GW 405833 exhibited the lowest intrinsic relative activity in the [^{35}S]GTPγS assay (E_{max}/EC_{50} = 0.10) but the highest activity in the cAMP assay (E_{max}/EC_{50} = 12.36). This pronounced shift indicates that the pharmacological profile of GW 405833 is highly dependent on the signalling endpoint measured and is consistent with pathway-dependent signalling. However, these findings should not be interpreted as definitive evidence of biased agonism, as formal bias assessment requires quantitative comparison across multiple pathways relative to a reference agonist, which was beyond the scope of this study.

In comparison with GW 405833, (R)-AM 1241 maintained a relatively stable rank order across assays, ranking third in the [^{35}S]GTPγS assay (E_{max}/EC_{50} = 1.57) and second in the cAMP assay (E_{max}/EC_{50} = 6.90). This suggests that its pharmacological behaviour is less influenced by downstream amplification than that of GW 405833. In recombinant systems, both (R)-AM 1241 and GW 405833 have been characterised as protean agonists, displaying agonist or inverse agonist activity depending on constitutive receptor activity. For example, suppression of constitutive CB_2R activity in CHO cells expressing recombinant human or rat CB_2 receptors, reveals the agonist properties of both compounds in cAMP assays [26]. These findings emphasise the dependence of protean agonist behaviour on cellular environment.

The ability of SR 144528, JTE 907, and AM 630 to reduce basal [^{35}S]GTPγS binding and enhance FSK-stimulated cAMP accumulation supports the presence of constitutively active CB_2Rs in BV-2 cells and is indicative of inverse agonist activity at this receptor population.

Both SR 144528 and AM 630 also displayed lower EC_{50} values than previously reported [30], indicating greater apparent potency under the present conditions, while maximal inverse agonist effects remained comparable. This suggests that ligand efficacy is broadly conserved, whereas apparent potency may depend on receptor expression, constitutive activity, and cellular signalling context.

Previous studies have shown that SR 144528 and AM 630 act as inverse agonists by preferentially stabilising the inactive state of CB_2R and reducing constitutive activity [30,44]. The present results are consistent with this mechanism, although the relative contributions of receptor expression and constitutive CB_2R activity were not directly assessed. Overall, BV-2 microglial cells provide a useful model for investigating agonism, protean agonism, and inverse agonism at CB_2Rs under non-inflammatory conditions, offering insight into CB_2R signalling in quiescent microglia.

Microglial activation is commonly described as a transition from homeostatic M0 cells towards a pro-inflammatory M1 phenotype, although CB_2R expression may increase or decrease depending on the type and severity of the inflammatory stimulus [8]. Endocannabinoids and exogenous cannabinoid agonists have also been reported to promote anti-inflammatory M2 polarisation. M2 microglia can produce 2-arachidonoylglycerol (2-AG) after interleukin-4 (IL-4) and interleukin-13 (IL-13) stimulation, while transforming growth factor-β (TGF-β) enhances anandamide (AEA) production [4,8]. These findings suggest a reciprocal relationship between endocannabinoid signalling and anti-inflammatory microglial responses.

In neurodegenerative disorders, modulation of the M1-M2 balance may be beneficial or detrimental depending on disease stage [2]. Suppression of M1 responses may reduce neuroinflammation and tissue damage during early or active diseases, whereas excessive or prolonged M2-associated activity could impair host defence or alter tissue remodelling. Therefore, the therapeutic effects of CB_2R ligands are likely to depend on their pharmacological properties, timing of intervention, and the prevailing microglial activation state.

Animal models of neuroinflammation consistently show marked CB_2R upregulation in activated microglia [7]. Thus, responses observed in non-stimulated BV-2 cells may not fully reflect those occurring under neuroinflammatory conditions, where receptor expression and signalling are shaped by a dynamic inflammatory environment. In addition, in vivo microglia rarely adopt purely M1 or M2 phenotypes but instead display heterogeneous activation states with simultaneous expression of M1- and M2-associated markers [45]. Consequently, CB_2R-mediated effects are likely to depend on microglial phenotype, local inflammatory conditions, and disease stage, highlighting the need for caution when extrapolating from simplified cellular models to in vivo settings [3].

The distinct pharmacological profiles identified here may inform future studies examining how CB_2R ligands regulate microglial responses under pathological conditions. Studies in activated microglia and in vivo models will be needed to determine whether these assay-dependent differences translate into distinct functional effects during disease.

Among the compounds tested, SR 144528 may be particularly useful for probing CB_2R function in non-stimulated microglia. It showed the greatest inverse agonist efficacy in the cAMP assay, indicating strong suppression of constitutive CB_2R signalling. SR 144528 also has one of the most selective binding profiles among commonly used cannabinoid ligands, with the fewest off-target interactions in a panel of 64 proteins associated with adverse human effects [39]. This selectivity supports its use as a tool for distinguishing CB_2R-mediated effects from broader cannabinoid pharmacology.

Previous studies have shown that SR 144528 reduces interleukin-10 (IL-10), a marker of M2 polarisation, in primary murine microglia exposed to pro-inflammatory stimuli [46]. It also partially inhibited anandamide-induced ERK1/2 and JNK phosphorylation, suggesting actions beyond simple CB_2R antagonism. Furthermore, SR 144528 has been reported to display signalling bias by antagonising 2-AG-induced Ca^{2+} mobilisation, reversing agonist-induced CB_2R internalisation, and increasing receptor surface expression [47]. These findings indicate that CB_2R modulation can involve selective regulation of signalling pathways, receptor trafficking, and receptor states.

Collectively, these observations highlight the complexity of CB_2R pharmacology and support the possibility of selectively targeting downstream CB_2R signalling. Ligands that preferentially engage beneficial anti-inflammatory pathways while minimising undesirable responses may improve the therapeutic potential of CB_2R-targeting compounds in neuroinflammatory and neurodegenerative disorders.

Several limitations should be considered. Although the observed responses were consistent with CB_2R-mediated signalling and known ligand profiles, receptor specificity was not confirmed using antagonist/inverse agonist blockade or genetic approaches, so off-target mechanisms cannot be excluded. CB_2R expression was also not directly quantified in the BV-2 cultures used, although basal expression in non-stimulated BV-2 cells has been demonstrated by RT-qPCR and Western blotting [48,49]. Future studies combining functional pharmacology with direct receptor quantification would therefore be valuable.

This study was performed only in non-stimulated BV-2 cells and does not address how inflammatory activation alters CB_2R expression or ligand responsiveness, both of which are known to change during microglial activation and neuroinflammation [8]. Although cells were maintained within a defined passage range, the influence of passage number was not directly assessed, despite evidence that prolonged passaging can alter gene expression, signalling pathways, protein expression, and cellular responsiveness [50]. In addition, BV-2 cells do not fully reproduce the transcriptional and phenotypic characteristics of primary microglia in vivo, although they remain a well-established and tractable model for mechanistic studies of microglial and cannabinoid receptor pharmacology [27,28].

Finally, differences between the [^{35}S]GTPγS and cAMP assays should be interpreted according to the signalling events measured. [^{35}S]GTPγS binding provides a relatively direct assessment of receptor-mediated G-protein activation, whereas cAMP accumulation reflects a downstream endpoint influenced by signal amplification and regulatory mechanisms. Thus, assay-dependent ligand activity may reflect receptor-level mechanisms, constitutive CB_2R activity, and downstream signalling processes. Future studies incorporating receptor blockade, genetic models, quantitative pathway analyses, activated microglia, and primary or in vivo systems will further clarify CB_2R pharmacology and the mechanisms underlying the ligand-dependent responses described here.

5. Conclusions

In conclusion, therapeutic manipulation of microglia in CNS disorders remains challenging due to the remarkable complexity of microglial biology, the dynamic nature of microglial phenotypes, and the incomplete understanding of microglial diversity across disease conditions, brain regions, age groups, and sexes. While most studies have focused on activated microglia, our data indicate that non-stimulated microglia represent a valuable and underexplored experimental model for investigating CB_2R pharmacology. Characterization of CB_2R ligands under basal conditions may help disentangle receptor-mediated effects from the numerous confounding factors associated with inflammatory activation, thereby providing novel insights into the role of the endocannabinoid system in microglial function and its potential therapeutic exploitation in CNS diseases [51,52].

Our data indicate that future studies should focus on characterizing the pharmacological effects of SR 144528 in BV-2 microglia polarized towards M1 and M2 phenotypes. Given its distinct potency and efficacy profile, evaluating its activity under different polarization states may provide further insight into the role of CB_2 receptor signalling in regulating microglial function and phenotype-dependent responses.

They also indicate special attention should be paid to the selection of experimental models that reflect distinct stages of disease progression, i.e., M polarization, as well as to the timing of treatment, since the consequences of microglial modulation are likely to vary according to the pathological context and disease stage.

Supplementary Materials: The following supporting information can be downloaded at https://www.mdpi.com/article/10.3390/targets4030031/s1: Table S1: GTPγS, agonists/proteans; Table S2: GTPγS, inverse agonists; Table S3: cAMP, agonists/proteans; Table S4: cAMP, inverse agonists.

Author Contributions: Conceptualization, P.M., P.T. and G.S.B.; methodology, P.M.; software, P.M.; validation, P.M., P.T. and S.S.; formal analysis, P.M.; investigation, P.M.; resources, P.T., M.G.M. and S.S.; data curation, P.M.; writing—original draft preparation, P.M.; writing—review and editing, P.T., G.S.B., M.G.M., S.S. and P.M.; visualization, P.M.; supervision, P.T. and G.S.B. All authors have read and agreed to the published version of the manuscript.

Funding: This research received no external funding.

Institutional Review Board Statement: Not applicable

Informed Consent Statement: Not applicable

Data Availability Statement: The original contributions presented in this study are included in the article/Supplementary Materials. Further inquiries can be directed to the corresponding author.

Acknowledgments: During the preparation of this manuscript, the authors used Gemini (July 2026 version) for the purposes of identifying typographical errors, refining text readability, and adapting table formatting. After using this tool, the authors reviewed and edited the output as needed and take full responsibility for the content of this publication.

Conflicts of Interest: The authors declare no conflicts of interest.

Abbreviations

The following abbreviations are used in this manuscript:

AM 630	6-iodopravadoline
CP 55,940	(−)-cis-3-[2-hydroxy-4-(1,1-dimethylheptyl)phenyl]-trans-4-(3-hydroxypropyl) cyclohexanol
DMSO	dimethyl sulphoxide
Forskolin (FSK)	7β-Acetoxy-8,13-epoxy-1α,6β,9α-trihydroxylabd-14-en-11-one
G418	3,5-dihydroxy-5-methyl-4-methylaminooxan-2-yl[oxy-2-hydroxycyclohexyl]oxy-2-(1-hydroxyethyl)oxane-3,4-diol
GW 405833	1-(2,3-dichlorobenzoyl)-5-methoxy-2-methyl-3-(2-(morpholin-4-yl)ethyl)-1H-indole hydrochloride
JTE 907	N-(1,3-benzodioxol-5-ylmethyl)-1,2-dihydro-7-methoxy-2-oxo-8-(pentyloxy)-3-quinolinecarboxamide
JWH 015	(2-methyl-1-propyl-1H-indol-3-yl)-1-naphthalenylmethanone
JWH 133	3-(1,1-dimethylbutyl)-1-deoxy-Δ8-tetrahydrocannabinol
PMSF	phenylmethylsulphonyl fluoride
(R)-AM 1241	(R,S)-3-(2-iodo-5-nitrobenzoyl)-1-(1-methyl-2-piperidinylmethyl)-1H-indole
SR 144528	N-[(1S)-endo-1,3,3-trimethylbicyclo[2.2.1]heptan-2-yl]-5-(4-chloro-3-methylphenyl)-1-(4-methylbenzyl)-pyrazole-3-carboxamide
WIN 55,212-2	(R)-(+)-[2,3-dihydro-5-methyl-3-(4-morpholinylmethyl)pyrrolo[1,2,3-de]-1,4-benzoxazin-6-yl]-1-naphthalenylmethanone mesylate

References

1. Young, A.P.; Denovan-Wright, E.M. The Dynamic Role of Microglia and the Endocannabinoid System in Neuroinflammation. *Front. Pharmacol.* **2022**, *12*, 806417. [CrossRef] [PubMed]
2. Šimončičová, E.; Gonçalves de Andrade, E.; Vecchiarelli, H.A.; Awogbindin, I.O.; Delage, C.I.; Tremblay, M.-È. Present and Future of Microglial Pharmacology. *Trends Pharmacol. Sci.* **2022**, *43*, 669–685. [CrossRef] [PubMed]
3. Fumagalli, L.; Nazlie Mohebiany, A.; Premereur, J.; Polanco Miquel, P.; Bijnens, B.; Van De Walle, P.; Fattorelli, N.; Mancuso, R. Microglia Heterogeneity, Modeling and Cell-State Annotation in Development and Neurodegeneration. *Nat. Neurosci.* **2025**, *28*, 1381–1392. [CrossRef] [PubMed]
4. Mecha, M.; Feliú, A.; Carrillo-Salinas, F.J.; Rueda-Zubiaurre, A.; Ortega-Gutiérrez, S.; de Sola, R.G.; Guaza, C. Endocannabinoids Drive the Acquisition of an Alternative Phenotype in Microglia. *Brain Behav. Immun.* **2015**, *49*, 233–245. [CrossRef] [PubMed]
5. Tanaka, M.; Sackett, S.; Zhang, Y. Endocannabinoid Modulation of Microglial Phenotypes in Neuropathology. *Front. Neurol.* **2020**, *11*, 87. [CrossRef] [PubMed]

6. Duffy, S.S.; Hayes, J.P.; Fiore, N.T.; Moalem-Taylor, G. The Cannabinoid System and Microglia in Health and Disease. *Neuropharmacology* **2021**, *190*, 108555. [CrossRef] [PubMed]
7. Kelly, R.; Joers, V.; Tansey, M.G.; McKernan, D.P.; Dowd, E. Microglial Phenotypes and Their Relationship to the Cannabinoid System: Therapeutic Implications for Parkinson's Disease. *Molecules* **2020**, *25*, 453. [CrossRef] [PubMed]
8. Komorowska-Müller, J.A.; Schmöle, A.-C. CB2 Receptor in Microglia: The Guardian of Self-Control. *Int. J. Mol. Sci.* **2021**, *22*, 19. [CrossRef] [PubMed]
9. Concannon, R.M.; Okine, B.N.; Finn, D.P.; Dowd, E. Differential Upregulation of the Cannabinoid CB_2 Receptor in Neurotoxic and Inflammation-Driven Rat Models of Parkinson's Disease. *Exp. Neurol.* **2015**, *269*, 133–141. [CrossRef] [PubMed]
10. Palazuelos, J.; Aguado, T.; Pazos, M.R.; Julien, B.; Carrasco, C.; Resel, E.; Sagredo, O.; Benito, C.; Romero, J.; Azcoitia, I.; et al. Microglial CB2 Cannabinoid Receptors Are Neuroprotective in Huntington's Disease Excitotoxicity. *Brain* **2009**, *132*, 3152–3164. [CrossRef] [PubMed]
11. Shoemaker, J.L.; Seely, K.A.; Reed, R.L.; Crow, J.P.; Prather, P.L. The CB2 Cannabinoid Agonist AM-1241 Prolongs Survival in a Transgenic Mouse Model of Amyotrophic Lateral Sclerosis When Initiated at Symptom Onset. *J. Neurochem.* **2007**, *101*, 87–98. [CrossRef] [PubMed]
12. Kosar, M.; Sarott, R.C.; Sykes, D.A.; Viray, A.E.G.; Vitale, R.M.; Tomašević, N.; Li, X.; Ganzoni, R.L.Z.; Kicin, B.; Reichert, L.; et al. Flipping the GPCR Switch: Structure-Based Development of Selective Cannabinoid Receptor 2 Inverse Agonists. *ACS Cent. Sci.* **2024**, *10*, 956–968. [CrossRef] [PubMed]
13. Han, Q.; Shao, Q.; Wang, X.; Ma, K.; Chen, N.; Yuan, Y. CB2 Receptor Activation Inhibits the Phagocytic Function of Microglia through Activating ERK/AKT-Nurr1 Signal Pathways. *Acta Pharmacol. Sin.* **2022**, *43*, 2253–2266. [CrossRef] [PubMed]
14. Lourbopoulos, A.; Grigoriadis, N.; Lagoudaki, R.; Touloumi, O.; Polyzoidou, E.; Mavromatis, I.; Tascos, N.; Breuer, A.; Ovadia, H.; Karussis, D.; et al. Administration of 2-Arachidonoylglycerol Ameliorates Both Acute and Chronic Experimental Autoimmune Encephalomyelitis. *Brain Res.* **2011**, *1390*, 126–141. [CrossRef] [PubMed]
15. Ehrhart, J.; Obregon, D.; Mori, T.; Hou, H.; Sun, N.; Bai, Y.; Klein, T.; Fernandez, F.; Tan, J.; Shytle, D. Stimulation of Cannabinoid Receptor 2 (CB2) Suppresses Microglial Activation. *J. Neuroinflam.* **2005**, *2*, 29. [CrossRef] [PubMed]
16. Shiratsuchi, A.; Watanabe, I.; Yoshida, H.; Nakanishi, Y. Involvement of Cannabinoid Receptor CB2 in Dectin-1-Mediated Macrophage Phagocytosis. *Immunol. Cell Biol.* **2008**, *86*, 179–184. [CrossRef] [PubMed]
17. Mecha, M.; Carrillo-Salinas, F.J.; Feliú, A.; Mestre, L.; Guaza, C. Microglia Activation States and Cannabinoid System: Therapeutic Implications. *Pharmacol. Ther.* **2016**, *166*, 40–55. [CrossRef] [PubMed]
18. Knopman, D.S.; Amieva, H.; Petersen, R.C.; Chételat, G.; Holtzman, D.M.; Hyman, B.T.; Nixon, R.A.; Jones, D.T. Alzheimer Disease. *Nat. Rev. Dis. Primers* **2021**, *7*, 33. [CrossRef] [PubMed]
19. Munro, S.; Thomas, K.L.; Abu-Shaar, M. Molecular Characterization of a Peripheral Receptor for Cannabinoids. *Nature* **1993**, *365*, 61–65. [CrossRef] [PubMed]
20. Pertwee, R.G.; Howlett, A.C.; Abood, M.E.; Alexander, S.P.H.; Marzo, V.D.; Elphick, M.R.; Greasley, P.J.; Hansen, H.S.; Kunos, G.; Mackie, K.; et al. International Union of Basic and Clinical Pharmacology. LXXIX. Cannabinoid Receptors and Their Ligands: Beyond CB1 and CB2. *Pharmacol. Rev.* **2010**, *62*, 588–631. [CrossRef] [PubMed]
21. Marini, P.; Cascio, M.-G.; King, A.; Pertwee, R.G.; Ross, R.A. Characterization of Cannabinoid Receptor Ligands in Tissues Natively Expressing Cannabinoid CB2 Receptors: Native CB2 Receptor Pharmacology. *Br. J. Pharmacol.* **2013**, *169*, 887–899. [CrossRef] [PubMed]
22. Kenakin, T. Inverse, Protean, and Ligand-Selective Agonism: Matters of Receptor Conformation. *FASEB J.* **2001**, *15*, 598–611. [CrossRef] [PubMed]
23. Min, A.D.; Matera, C.; Bock, A.; Holze, J.; Kloeckner, J.; Muth, M.; Traenkle, C.; Amici, M.D.; Kenakin, T.; Holzgrabe, U.; et al. A New Molecular Mechanism To Engineer Protean Agonism at a G Protein–Coupled Receptor. *Mol. Pharmacol.* **2017**, *91*, 348–356. [CrossRef] [PubMed]
24. Bolognini, D.; Cascio, M.G.; Parolaro, D.; Pertwee, R.G. AM630 Behaves as a Protean Ligand at the Human Cannabinoid CB2 Receptor. *Br. J. Pharmacol.* **2012**, *165*, 2561–2574. [CrossRef] [PubMed]
25. Yao, B.B.; Mukherjee, S.; Fan, Y.; Garrison, T.R.; Daza, A.V.; Grayson, G.K.; Hooker, B.A.; Dart, M.J.; Sullivan, J.P.; Meyer, M.D. In Vitro Pharmacological Characterization of AM1241: A Protean Agonist at the Cannabinoid CB2 Receptor? *Br. J. Pharmacol.* **2006**, *149*, 145–154. [CrossRef] [PubMed]
26. Mancini, I.; Brusa, R.; Quadrato, G.; Foglia, C.; Scandroglio, P.; Silverman, L.S.; Tulshian, D.; Reggiani, A.; Beltramo, M. Constitutive Activity of Cannabinoid-2 (CB2) Receptors Plays an Essential Role in the Protean Agonism of (+)AM1241 and L768242. *Br. J. Pharmacol.* **2009**, *158*, 382–391. [CrossRef] [PubMed]
27. Henn, A. The Suitability of BV2 Cells as Alternative Model System for Primary Microglia Cultures or for Animal Experiments Examining Brain Inflammation. *ALTEX* **2009**, *26*, 83–94. [CrossRef] [PubMed]

28. Horvath, R.J.; Nutile-McMenemy, N.; Alkaitis, M.S.; DeLeo, J.A. Differential Migration, LPS-Induced Cytokine, Chemokine, and NO Expression in Immortalized BV-2 and HAPI Cell Lines and Primary Microglial Cultures. *J. Neurochem.* **2008**, *107*, 557–569. [CrossRef] [PubMed]
29. Peng, Y.; Chu, S.; Yang, Y.; Zhang, Z.; Pang, Z.; Chen, N. Neuroinflammatory In Vitro Cell Culture Models and the Potential Applications for Neurological Disorders. *Front. Pharmacol.* **2021**, *12*, 671734. [CrossRef] [PubMed]
30. Ross, R.A.; Brockie, H.C.; Stevenson, L.A.; Murphy, V.L.; Templeton, F.; Makriyannis, A.; Pertwee, R.G. Agonist-Inverse Agonist Characterization at CB1 and CB2 Cannabinoid Receptors of L759633, L759656, and AM630. *Br. J. Pharmacol.* **1999**, *126*, 665–672. [CrossRef] [PubMed]
31. Vasavda, C.; Zaccor, N.W.; Scherer, P.C.; Sumner, C.J.; Snyder, S.H. Measuring G-protein-coupled Receptor Signaling via Radio-labeled GTP Binding. *JoVE (J. Vis. Exp.)* **2017**, *124*, e55561. [CrossRef] [PubMed]
32. Devane, W.A.; Dysarz, F.A.; Johnson, M.R.; Melvin, L.S.; Howlett, A.C. Determination and Characterization of a Cannabinoid Receptor in Rat Brain. *Mol. Pharmacol.* **1988**, *34*, 605–613. [CrossRef]
33. Eissenstat, M.A.; Bell, M.R.; D'Ambra, T.E.; Alexander, E.J.; Daum, S.J.; Ackerman, J.H.; Gruett, M.D.; Kumar, V.; Estep, K.G.; Olefirowicz, E.M. Aminoalkylindoles: Structure-Activity Relationships of Novel Cannabinoid Mimetics. *J. Med. Chem.* **1995**, *38*, 3094–3105. [CrossRef] [PubMed]
34. Kurkinen, K.M.; Koistinaho, J.; Laitinen, J.T. [Gamma-35S]GTP Autoradiography Allows Region-Specific Detection of Muscarinic Receptor-Dependent G-Protein Activation in the Chick Optic Tectum. *Brain Res.* **1997**, *769*, 21–28. [CrossRef] [PubMed]
35. Breivogel, C.S.; Griffin, G.; Di Marzo, V.; Martin, B.R. Evidence for a New G Protein-Coupled Cannabinoid Receptor in Mouse Brain. *Mol. Pharmacol.* **2001**, *60*, 155–163. [CrossRef]
36. Marini, P.; Cascio, M.G.; Pertwee, R.G. The Cyclic AMP Assay Using Human Cannabinoid CB2 Receptor-Transfected Cells. *Methods Mol. Biol.* **2016**, *1412*, 85–93. [CrossRef] [PubMed]
37. Tucci, P.; Brown, I.; Bewick, G.S.; Pertwee, R.G.; Marini, P. The Plant Derived 3-3′-Diindolylmethane (DIM) Behaves as CB2 Receptor Agonist in Prostate Cancer Cellular Models. *Int. J. Mol. Sci.* **2023**, *24*, 3620. [CrossRef] [PubMed]
38. Harrison, C.; Traynor, J.R. The [35S]GTPγS Binding Assay: Approaches and Applications in Pharmacology. *Life Sci.* **2003**, *74*, 489–508. [CrossRef] [PubMed]
39. Soethoudt, M.; Grether, U.; Fingerle, J.; Grim, T.W.; Fezza, F.; de Petrocellis, L.; Ullmer, C.; Rothenhäusler, B.; Perret, C.; van Gils, N.; et al. Cannabinoid CB2 Receptor Ligand Profiling Reveals Biased Signalling and Off-Target Activity. *Nat. Commun.* **2017**, *8*, 13958. [CrossRef] [PubMed]
40. Pietr, M.; Kozela, E.; Levy, R.; Rimmerman, N.; Lin, Y.H.; Stella, N.; Vogel, Z.; Juknat, A. Differential Changes in GPR55 during Microglial Cell Activation. *FEBS Lett.* **2009**, *583*, 2071–2076. [CrossRef] [PubMed]
41. Xia, R.; Yuan, Q.; Wang, N.; Hou, L.; Abe, J.; Song, J.; Ito, Y.; Xu, H.E.; He, Y. Structural Insight into GPR55 Ligand Recognition and G-Protein Coupling. *Cell Res.* **2025**, *35*, 76–79. [CrossRef] [PubMed]
42. Zhang, R.; Kavana, M. Quantitative Measure of Receptor Agonist and Modulator Equi-Response and Equi-Occupancy Selectivity. *Sci. Rep.* **2016**, *6*, 25158. [CrossRef] [PubMed]
43. Strange, P.G. Use of the GTPγS ([35S]GTPγS and Eu-GTPγS) Binding Assay for Analysis of Ligand Potency and Efficacy at G Protein-Coupled Receptors. *Br. J. Pharmacol.* **2010**, *161*, 1238–1249. [CrossRef] [PubMed]
44. Rinaldi-Carmona, M.; Barth, F.; Millan, J.; Derocq, J.-M.; Casellas, P.; Congy, C.; Oustric, D.; Sarran, M.; Bouaboula, M.; Calandra, B.; et al. SR 144528, the First Potent and Selective Antagonist of the CB2 Cannabinoid Receptor. *J. Pharmacol. Exp. Ther.* **1998**, *284*, 644–650. [CrossRef]
45. Martinez, F.O.; Gordon, S. The M1 and M2 Paradigm of Macrophage Activation: Time for Reassessment. *F1000Prime Rep.* **2014**, *6*, 13. [CrossRef] [PubMed]
46. Correa, F.; Hernangómez, M.; Mestre, L.; Loría, F.; Spagnolo, A.; Docagne, F.; Di Marzo, V.; Guaza, C. Anandamide Enhances IL-10 Production in Activated Microglia by Targeting CB_2 Receptors: Roles of ERK1/2, JNK, and NF-κB: Anandamide Enhances IL-10 Production. *Glia* **2010**, *58*, 135–147. [CrossRef] [PubMed]
47. Mallipeddi, S.; Janero, D.R.; Zvonok, N.; Makriyannis, A. Functional Selectivity at G-Protein Coupled Receptors: Advancing Cannabinoid Receptors as Drug Targets. *Biochem. Pharmacol.* **2017**, *128*, 1–11. [CrossRef] [PubMed]
48. Shan, R.; Zhang, Y.; Shi, Y.; Wang, X.; Wang, X.; Ma, G.; Li, Q. Activation of Cannabinoid Type 2 Receptor in Microglia Reduces Neuroinflammation through Inhibiting Aerobic Glycolysis to Relieve Hypertension. *Biomolecules* **2024**, *14*, 333. [CrossRef] [PubMed]
49. Grabon, W.; Ruiz, A.; Gasmi, N.; Degletagne, C.; Georges, B.; Belmeguenai, A.; Bodennec, J.; Rheims, S.; Marcy, G.; Bezin, L. CB2 Expression in Mouse Brain: From Mapping to Regulation in Microglia under Inflammatory Conditions. *J. Neuroinflam.* **2024**, *21*, 206. [CrossRef] [PubMed]
50. Liu, S.; Peng, H.; Meng, J.; Zhuo, L.; Fu, S.; Yang, W. Cell Passage Number Drives Transcriptomic Drift as an Overlooked Factor in Experimental Reproducibility. *Sci. Rep.* **2025**, *15*, 44984. [CrossRef] [PubMed]

51. Spinelli, F.; Mu, L.; Ametamey, S.M. Radioligands for Positron Emission Tomography Imaging of Cannabinoid Type 2 Receptor. *J. Label. Compd. Radiopharm.* **2018**, *61*, 299–308. [CrossRef] [PubMed]
52. Ni, R.; Mu, L.; Ametamey, S. Positron Emission Tomography of Type 2 Cannabinoid Receptors for Detecting Inflammation in the Central Nervous System. *Acta Pharmacol. Sin.* **2019**, *40*, 351–357. [CrossRef] [PubMed]